Canadian Conference - Pacific Conference on Earthquake Engineering 2023

Vancouver, British Columbia

June 25th – June 30th, 2023

Structural parametric study on seismic response and higher mode effects mitigation of unbonded post-tensioned precast walls

Mahya Moghadasi[1*], Mohammad H Ahmadi[2], Fawad A Najam[3], Saeed Dehghani[4], Lisa Tobber[5]

[1]Ph.D. student, School of Engineering, The University of British Columbia-Okanagan
[2] Post-doctoral fellow, School of Engineering, The University of British Columbia-Okanagan
[3] Post-doctoral fellow, School of Engineering, The University of British Columbia-Okanagan
[4] Ph.D. student, School of Engineering, The University of British Columbia-Okanagan
[5] Assistant professor, School of Engineering, The University of British Columbia-Okanagan
[*]mahyam@student.ubc.ca

ABSTRACT

In high seismic regions, by population growth, the demand for resilient structures has led to the increasing popularity of precast (PC) construction. Generally, these systems are considered an economical and time-saving solution for constructing low-rise buildings. However, with recent developments in terms of improved connection details and enhanced energy dissipation mechanisms, precast wall systems are also gaining acceptance as effective lateral force-resisting systems for mid- to high-rise buildings in many parts of the world, such as New Zealand. In recent years, jointed precast concrete shear walls with energy dissipation devices and self-centering capabilities using unbonded post-tensioned tendons have become the preferred solution for building structures in high seismic regions. For conventional reinforced concrete shear walls, several studies have already quantified the effect of building height and other parameters on the relative contributions of individual vibration modes in the dynamic response. In contrast, there is still a lack of knowledge on the seismic performance of ductile PC walls with different types of connections. This study used a detailed parametric analysis scheme to investigate the higher-mode amplification effects in the seismic response of unbonded post-tensioned precast concrete (UPT-PC) wall systems. Since the lateral dynamic behavior of this system is mainly characterized by base rocking and self-centering mechanisms, several parameters, including strain hardening of the post-tensioned (PT) cables, PT initial force, and energy dissipation (ED), are considered. The nonlinear time history analysis is conducted on a 20-story building using a set of earthquake ground motions consistent with uniform hazard spectra for site class D in Vancouver, Canada. The results clearly identified the factors leading to significant contributions from higher modes in various engineering demand parameters. Improving ED is the most effective approach to mitigate the higher-mode effects in the structural response of UPT-PC walls.

Keywords: Unbonded post-tensioned precast walls, precast wall, Higher mode effects, Time history analysis, Parametric study

INTRODUCTION

In recent years, precast concrete structures have become increasingly popular in many countries due to their numerous benefits, including speed of construction, cost-effectiveness, superior quality components, and improved onsite safety. However, despite these advantages, some engineers have hesitated to use precast concrete structures because of concerns about their seismic performance. Several catastrophic earthquakes, such as the 1994 Northridge earthquake, the 1995 Kobe earthquake, and the Spitak earthquake in Armenia in 1988, have highlighted the vulnerability of precast concrete structural elements during seismic events [1,2], mainly due to improper connections between wall panels and foundations. As a result, there is a growing need for further research on the seismic performance of precast concrete structures, particularly for ductile systems utilized in high-rise buildings in high seismic regions.

Shear walls have garnered significant attention, particularly in Canada, due to their stiffness compared to other lateral resisting systems such as RC frames. Researchers have been exploring using precast walls specifically for ductile systems, which are crucial for high-rise buildings in high seismic areas. The demand for research in this area is rapidly increasing as engineers seek to enhance the seismic performance of precast concrete structures and make them more resilient to earthquakes.

Precast concrete structures are typically categorized into three main groups based on their connection type: jointed, emulative, and emulative transition. The jointed construction method, or the dry joint method, is further classified into two categories: limited ductility joints and ductile joints [3]. Numerous studies have been conducted on using ductile jointed precast walls with gap openings across horizontal connections using only unbonded post-tensioned steel [4-10]. However, it was discovered that these walls have limited energy dissipation capacity and suffer from excessive uplift, shear slip, and degradation in lateral strength and stiffness. This was due to the accumulation of plastic tensile strains in the connection during reversed-cyclic loading. The lack of energy dissipation capacity was related to the unbonded post-tensioned connections, which were designed not to yield during earthquakes. To address this weakness, researchers have investigated the use of mild steel reinforcement in addition to post-tensioned steel to provide flexural strength and inelastic energy dissipation. A precast hybrid wall specimen constructed in this manner is illustrated in Figure 1.

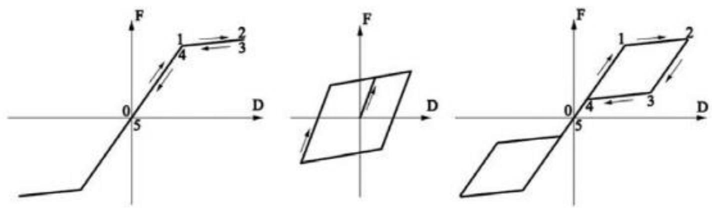

Figure 1. Hysteresis curve, a) Rocking wall without energy dissipaters, b) mild steel, c) Hybrid wall [11]

On the other hand, jointed precast concrete structures may also be susceptible to higher mode effects during seismic events. These effects occur when a structure's higher frequency vibration modes are excited by ground motion, causing a shift in the structure's fundamental period and potentially increasing its vulnerability to seismic damage. To address these challenges, researchers have been exploring various approaches to improve the seismic performance of jointed precast concrete structures, such as using multi segments or bi-rocking walls. They suggested reducing these effects by designing to allow rocking to occur at multiple locations over the height of a base-rocking system. [12-14].

This paper investigated the effects of various design parameters, including the strain hardening of PT tendons, the initial force of PT, and ED, on the higher modes of UPT-PC wall systems. The primary objective was to ascertain whether these parameters could effectively mitigate the higher mode effects. For this purpose, a 20-story RC wall was considered in Vancouver, Canada, for site class D under 15 earthquake records to conduct nonlinear time history analysis. By exploring the interplay between these critical factors, the study aimed to provide insights into optimizing the design of structures subjected to dynamic loads.

UNBONDED POST-TENSIONED PRECAST WALL SYSTEMS

As discussed in the previous section, hybrid walls by implementing a controlled rocking approach, such as a concentrated rotational mechanism at a suggested critical joint (for example, the base joint placed at the top of the foundation), most of the nonlinear axial-flexural deformations can be concentrated. The use of UPT cables provides an opportunity to have a rocking behavior, which is made by the opening and subsequent closing of the gap. Because of the concentrated rotations, minor damage occurs to the precast panel when a large nonlinear lateral displacement happens in the wall [15]. Figure 2 compares traditional walls with UPT-PC walls with and without energy dissipation.

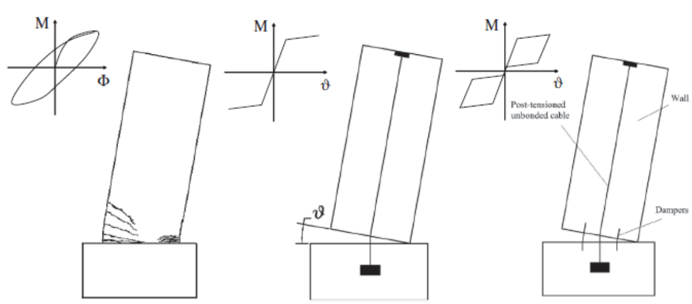

Figure 2. Comparison between responses of (a) traditional RC, (b) precast walls without additional dampers, and (c) precast walls with additional dampers [16]

The ED steel moment ratio, denoted by k_d, is defined by Equation (1) [17] and is used to quantify the proportion of UPT cables and ED devices in a hybrid wall system. The numerator and denominator of the equation represent energy dissipation and self-centering, respectively.

$$K_d = \frac{M_{ED}}{M_{PT}+M_w} \tag{1}$$

Where M_{PT} = moment provided by initial effective PT force; M_w = moment supplied by the applied (external) axial load; M_{ED}= maximum moment provided by the energy dissipating elements.

The contribution of re-centering and dissipation components can be varied to modify the shape and properties of the "flag-shape," as shown in Figure 3.

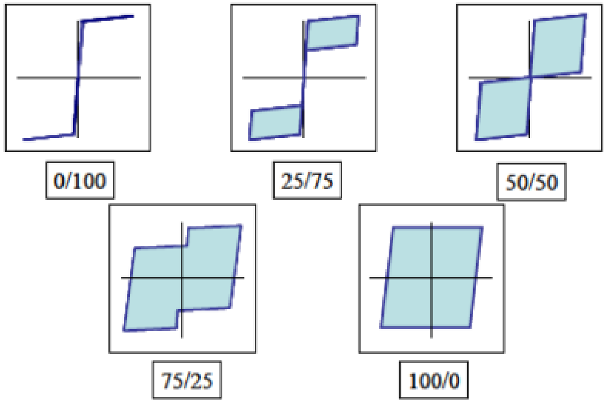

Figure 3: Effects of varying the ratio between re-centering (post-tensioning and axial load) vs. dissipative (mild steel and dissipaters) contribution to the Flag-Shape Hysteresis loop.[18]

An appropriate value for kd must be selected during the design phase to ensure sufficient energy dissipation and self-centering. If k_d is too small, the wall's energy dissipation capability may be inadequate, while a large k_d may lead to insufficient self-centering. To address this issue, Smith and Kurama [19] recommend a k_d ratio between 0.50 and 0.80 for optimal performance.

The flag-shaped characteristics of rocking wall systems can be identified by considering multiple factors [12]. Specifically, the decompression moment of the rocking section (M_{Decomp}), the moment at which the anchors yield, and the ED elements are fully yielded (M_y), and the ultimate moment of the system (Mu) are all critical in determining the system's behavior. The mathematical expressions for these variables are defined as follows. In Equation (2) β presents the term of energy dissipation, and L_w is the length of the wall. Figure 4 shows the existing loads schematically.

$$M_{Decomp} = \left(W + F_{PT_{in}}\right)\left(\frac{L_w}{2}\right) \tag{2}$$

$$M_y = \frac{W+F_{PT_{in}}}{1-\frac{\beta}{2}}\left(\frac{L_w}{2}\right) \tag{3}$$

$$M_u = M_y + M_{PT} \tag{4}$$

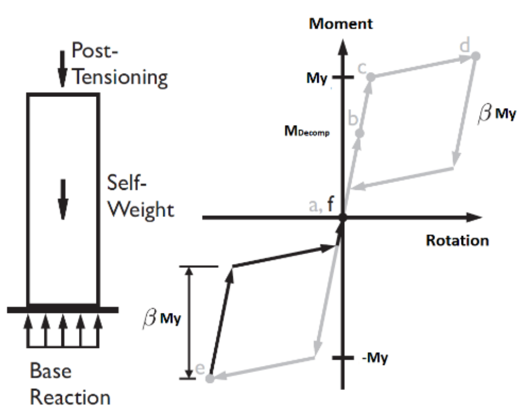

Figure 4. Free diagram and the response of base-rocking system [12].

STUDIED PARAMETERS

Structural parameters

This study aimed to assess the seismic behavior of a building with a UPT base connection. A parametric study was conducted on a 20-story building in Vancouver, Canada, with site class D. The prototype plan was chosen based on the Canadian Precast/Prestressed Concrete Institute (CPCI) design example [20] was a precast building plan. The dimensions of the plan $53m \times 19.6m$ were considered for all archetypes, as shown in Figure 5. One of the shear walls depicted in Figure 5 (W8) was selected for preliminary design as a UPT-PC wall for the parametric study. Table 1 presents the wall's cross-sectional geometry and material properties for the prototype building.

Table 1. Parameters of prototype building.

parameter	**20 story**
Total mass per floor(kN)	5940
Wall cross-sectional area (m^2)	2.59
Gross moment of inertia (m^4)	16.06
E_cI_g (kNm^2)	$4.3*10^8$
Wall length (m)	8.6
$\frac{\boldsymbol{w_g}}{\boldsymbol{A_g f'_c}}$	9.85%
$\boldsymbol{f'_c}$ (MPa)	35

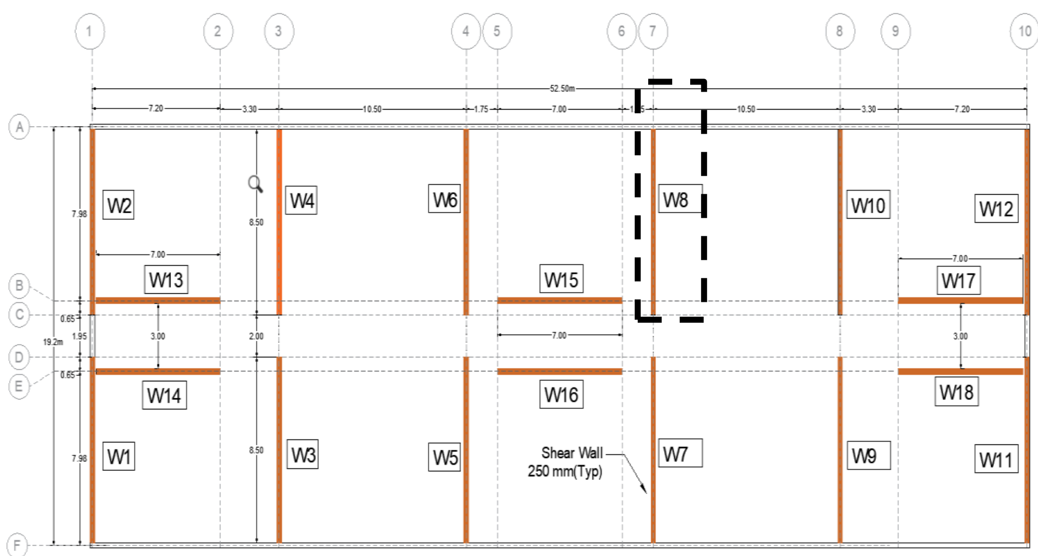

Figure 5. The concrete wall location plan of the prototype.

Considered UPT-PC walls

A wide range of UPT-PCs was considered in this paper for conducting a parametric study, evaluating the effect of the design parameters on higher mode effect mitigation in tall buildings. In Figure 6, reference models were classified using parameters α, β, and PT initial. Generally, the post-yield hardening ratio, α, and the ED ratio, β, were considered to range between 0% to 20% and 0% to 100%, respectively. Also, the initial PT force was assumed to be 0%, 7.5%, and 15% of the seismic mass. Totally, 36 archetypes were investigated in this paper.

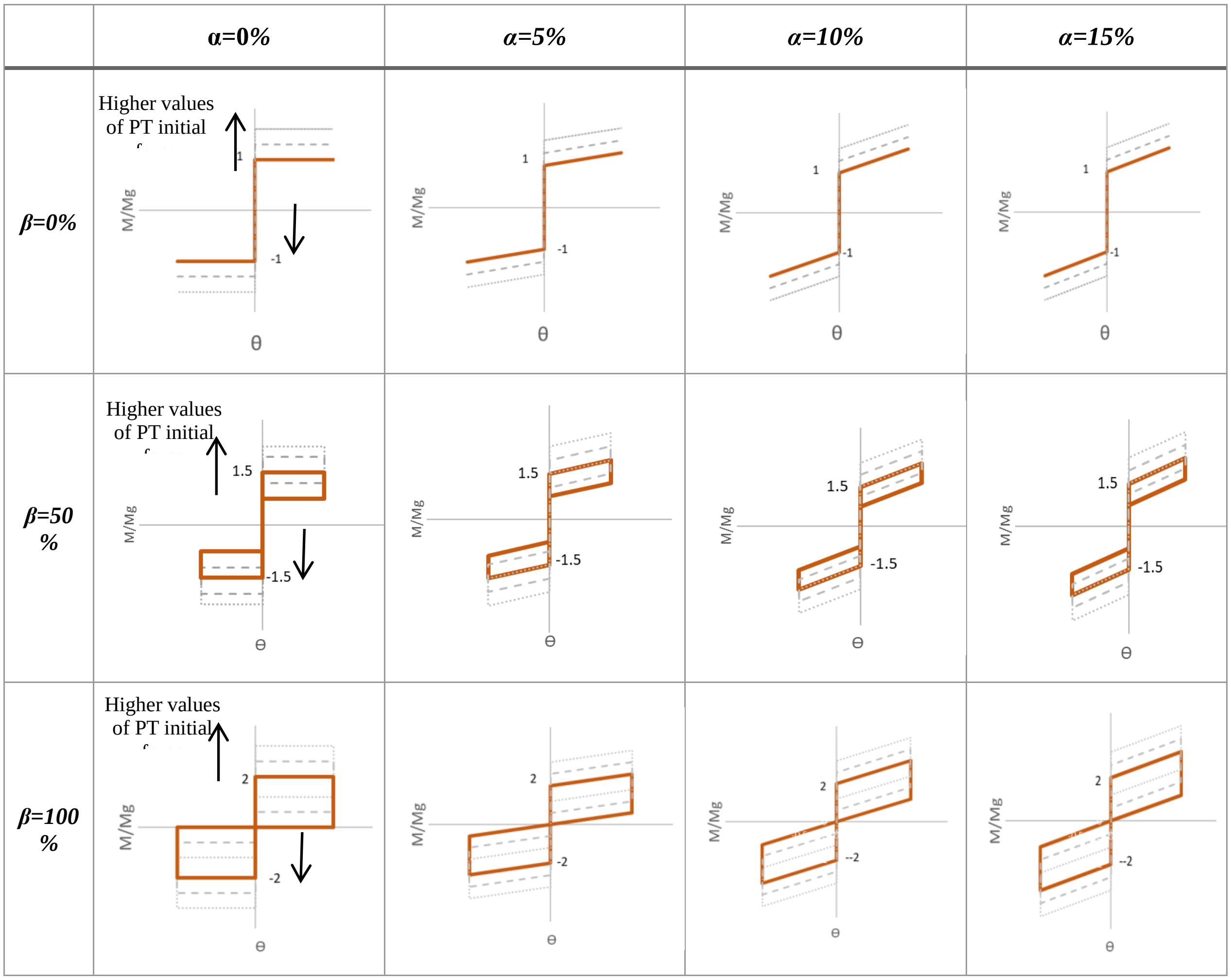

Figure 6. Force-displacement hysteretic models for self-centering earthquake-resisting systems (UPT-PCs)

Numerical modeling of the wall system

According to the previous section, to define the nonlinear behavior of the UPT-PC wall in the numerical modeling, the elastic wall was combined with the inelastic connection at the bottom of the wall, resulting in the flag-shaped behavior of the system, as shown in Figure 7. The system's initial stiffness (k) equals the elastic stiffness of the wall. As mentioned before, M_y and M_u are the system's yield moment and ultimate moment, respectively.

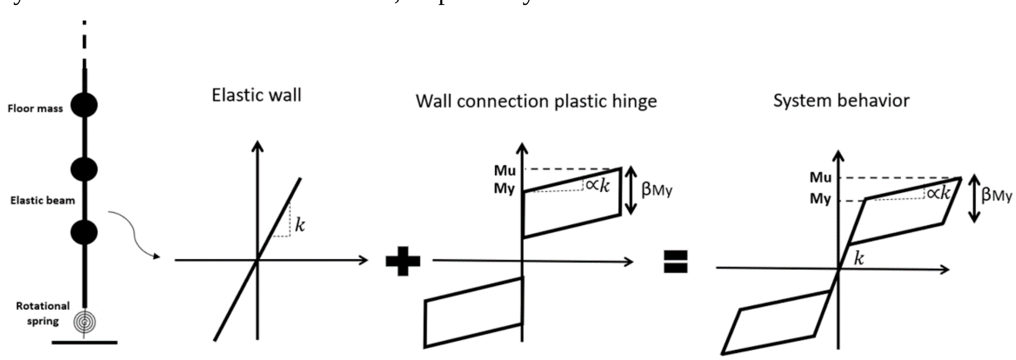

Figure 7. Numerical modeling concept.

The nonlinear analysis program, OPENSEES 3.3 [21], was used to simulate the UPT-PC wall system to calculate the nonlinear responses. The wall panels were considered as elastic elements using the elasticBeamColumn element; it should be noted that the concrete at the base of the wall remained linear. Therefore, it was a valid assumption in analysis to consider that the deformation in concrete was linear [12-14]. A Zero-Length rotational spring with a flag-shaped behavior was defined at the base of the wall. This behavior was assigned using Self-Centering material to model the nonlinear behavior corresponding to PT and ED. To show the elastic and inelastic behavior of the system in OPENSEES, a cyclic load is applied to the elastic wall, wall connection, and the system separately. Figure 8 illustrates the behavior of each component under cyclic loading.

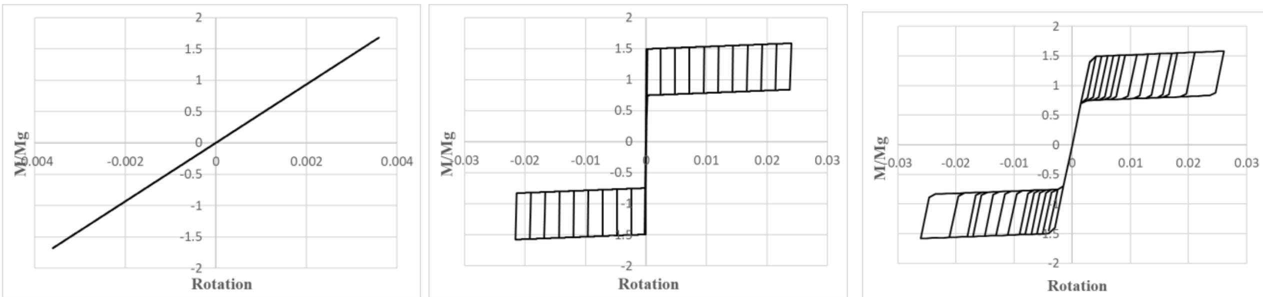

(a) *(b)* *(c)*

Figure 8. Hysteresis behavior of the system in OPENSEES: (a) Elastic wall (b) Wall connection plastic hinge (c) System

SELECTION AND SCALING OF GROUND MOTIONS

Design Spectrum and Scaling Method

In the 2020 NBCC, the design spectrum, S(T), is obtained from uniform hazard spectral ordinates calculated for a probability of exceedance of 2% in 50 years at periods of 0.2, 0.5, 1.0, 2.0, 5.0, and 10.0 s. For site class D in Vancouver, BC, these values are shown in Figure 9. Selection and scaling of ground motion time histories must be performed considering the design spectrum over a range of periods that extends between the periods equal to 0.2T1 and 1.5T1. The periods in the first three modes of vibrations are respectively equal to 1.5, 1.27, and 1.18s, and the 7^{th} mode was corresponding cumulated participating masses equal to 90% of the total structure mass. So, The lower bound of the period range was then equal to 0.225 s, and the upper limit was taken equal to 2.25 s.

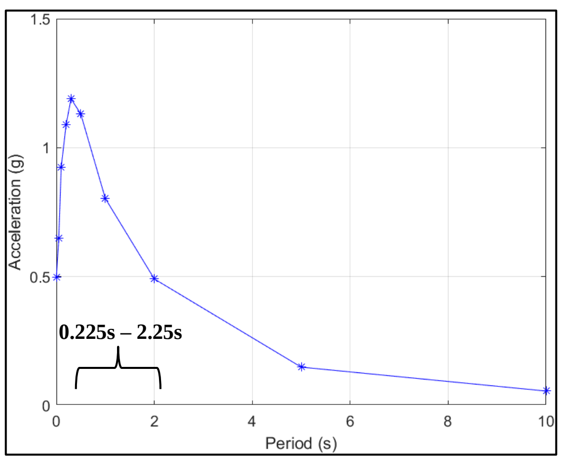

Figure 9. Design spectrum adopted for site class D, Vancouver, BC

Ground Motion Selection

The Time History Analyses utilized far-field ground motions on site class D, which consisted of 15 pairs of horizontal ground motions taken from 15 different earthquake events. These motions were used to apply to the flag-shaped models described in the previous section and obtained the exact inelastic responses. The FEMA P695[22] guideline recommends this set of far-field ground motions, considered a reliable sample of earthquake ground motions due to its ability to account for record-to-record variability in nonlinear dynamic analyses. The selection of records for this set is based on several criteria, including the number of records per event, moment magnitude values (Mw > 6.5), source and site conditions, source-to-site distance, peak ground acceleration range (PGAs > 0.2 g), and peak ground velocity range (PGVs > 15 cm/s). Table 2 summarizes the far-field records, and some of their seismological characteristics, and Figure 9 shows the scaled spectral acceleration of the records to the design spectrum, as well as their median response spectra.

Table 2. Selected earthquake records

	Name, Station	V_s (m/s)	Site Class	Fault	R (km)	M_w	PGA (g)
1	Northridge, Beverly Hills - Mulhol USC	356	D	Thrust	13.3	6.7	0.41
2	Duzce, Turkey Bolu ERD	326	D	Strike-slip	41.3	7.1	0.52
3	Imperial Valley, El Centro Array #11 US	196	D	Strike-slip	33.7	6.5	0.35
4	Kobe, Japan Shin-Osaka CUE	256	D	Strike-slip	46	6.9	0.24
5	Kocaeli, Turkey Duzce ERD	276	D	Strike-slip	98.2	7.5	0.31
6	Northridge, Canyon Country-WLC USC	309	D	Thrust	26.5	6.7	0.41
7	Loma Prieta, Gilroy Array #3 CDMG	350	D	Strike-slip	31.4	6.9	0.56
8	Superstition Hills, El Centro Imp. Co.	192	D	Strike-slip	35.8	6.5	0.36
9	Superstition Hills, Poe Road (temp) US	208	D	Strike-slip	11.2	6.5	0.43
10	Cape Mendocino, Rio Dell Overpass CDMG	312	D	Thrust	22.7	7	0.39
11	Chi-Chi, Taiwan CHY101 CWB	259	D	Thrust	32	7.6	0.31
12	San Fernando, LA - Hollywood Stor CDMG	316	D	Thrust	39.5	6.6	0.21
13	Imperial Valley, Delta UNAMUCSD	275	D	Strike-slip	33.7	6.5	0.21
14	Landers, Yermo Fire Station CDMG	354	D	Strike-slip	86	7.3	0.23
15	Loma Prieta, Capitola CDMG	289	D	Strike-slip	9.8	6.9	0.51

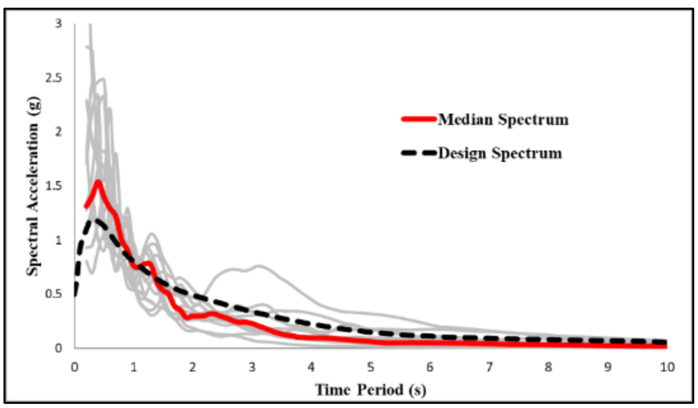

Figure 10. 5% damped acceleration spectra of the individual selected records after scaling.

RESULTS AND DISCUSSION

The results obtained are discussed and summarized with respect to the effects of higher modes and structural parameters on the UPT-PC wall responses. The mean distribution of the moment, shear forces, inter-story drifts, and acceleration demands caused by seismic records throughout the height of the 20-story building were compared considering three different structural parameters, α, β, and PT initial forces.

Drift

According to Figures 11 and 12, it was generally observed that the drift values of stories 1-8 in UPT-PC walls were significantly higher as compared to elastic shear walls. However, the drift decreased in stories 9-20 of UPT-PC walls rather than the elastic shear wall. This can be attributed to the inherent characteristics of the two structural systems and the rocking behavior in the UPT-PC wall. Another result was the uniform drift distribution in UPT-PC walls in comparison with the elastic wall due to their ability to undergo a certain amount of deformation under seismic loading. In lower stories of UPT-PC walls, the drift was distributed more uniformly across the height of the wall rather than in upper stories (higher than the 9th story). The PT tendons in the wall helped to distribute the deformation and dissipate the energy of the earthquake, resulting in a more even distribution of drift. It should be noted that the low amount of drift for fixed base structure is related to the elastic behavior assumption for the wall.

As shown in Figure 11, higher values of β result in considerably lower drifts in upper levels and more uniform drift distribution. Also, Figure 12 demonstrates that by increasing β from 0% to 100%, the maximum inter-story drift was reduced about 25%. The trend of the curves in Figure 12 shows that the effect of α and PT initial forces was not considerable. Moreover, the lowest drift among all archetypes belongs to the structure with β=100%, which equals about 0.6% with different α and PT initial forces.

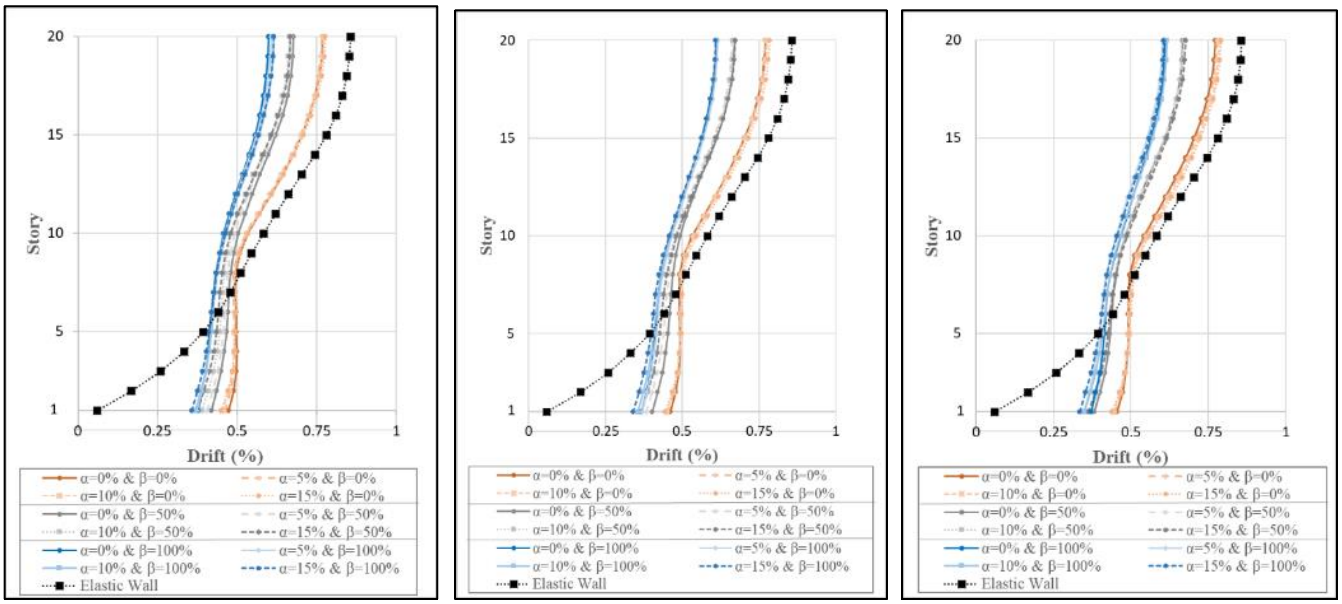

(a) *(b)* *(c)*

Figure 11. Comparing inter-story drift for all scenarios: (a) PT initial= 0%W; (b) PT initial= 7.5%W; (c) PT initial= 15%W

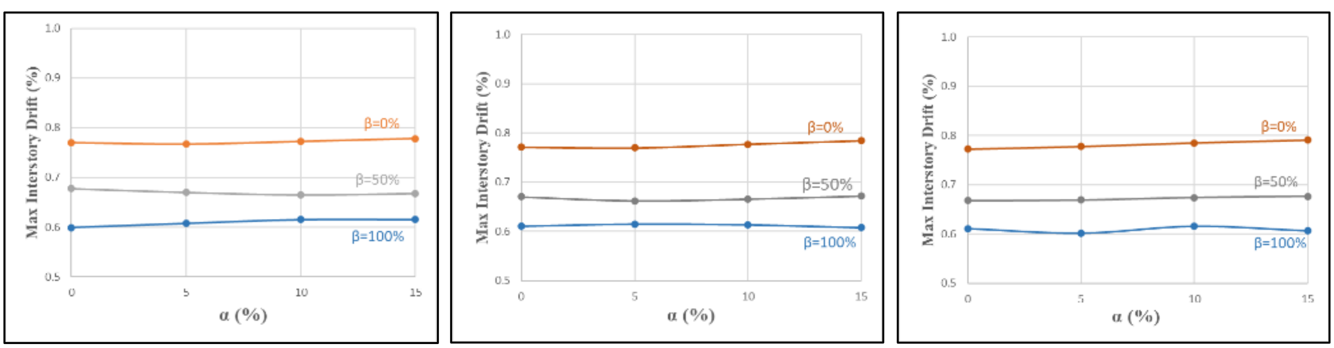

(a) *(b)* *(c)*

Figure 12. Comparing maximum inter-story drift for all archetypes; (a) PT initial= 0%W; (b) PT initial= 7.5%W; (c) PT initial= 15%W

Shear

In general, it can be observed that elastic shear walls may exhibit higher shear forces as compared to UPT-PC walls due to their higher stiffness and strength. Elastic shear walls are designed to resist the lateral forces caused by seismic events by developing shear forces in the walls, which are then transferred to the foundation. In contrast, UPT-PC walls are designed to dissipate the seismic energy through PT tendons and deformation, which results in a more distributed shear force distribution. PT tendons are designed to help distribute the shear forces more uniformly across the height of the wall.

According to Figure 13, the minimum and maximum reduction of the UPT-PC wall shear demands were 25% and 40% rather than the elastic shear wall with fixed connection. In UPT-PC walls, the shear distribution was rapidly reduced from the base to about the 9th story, while it increased first and then decreased from the 9th story to the 20th story. The peak value of shear envelopes in higher stories occurred at about the 17th story and was up to 80% of the weight. The highest values of shear forces in the base of all structures were mitigated by increasing the ED (β). Considering 50% or 100% for ED (β) decreased shear demand up to 15%. Two other parameters, α and PT initial forces, did not considerably influence the shear forces. In other words, Figure 14 shows a fluctuation regarding the effect of these parameters. Furthermore, the lowest shear demand among all archetypes belongs to the structure with β=100%, α=0%, and PT initial force=0%, which is equal to 11.5% of the weight of the structure.

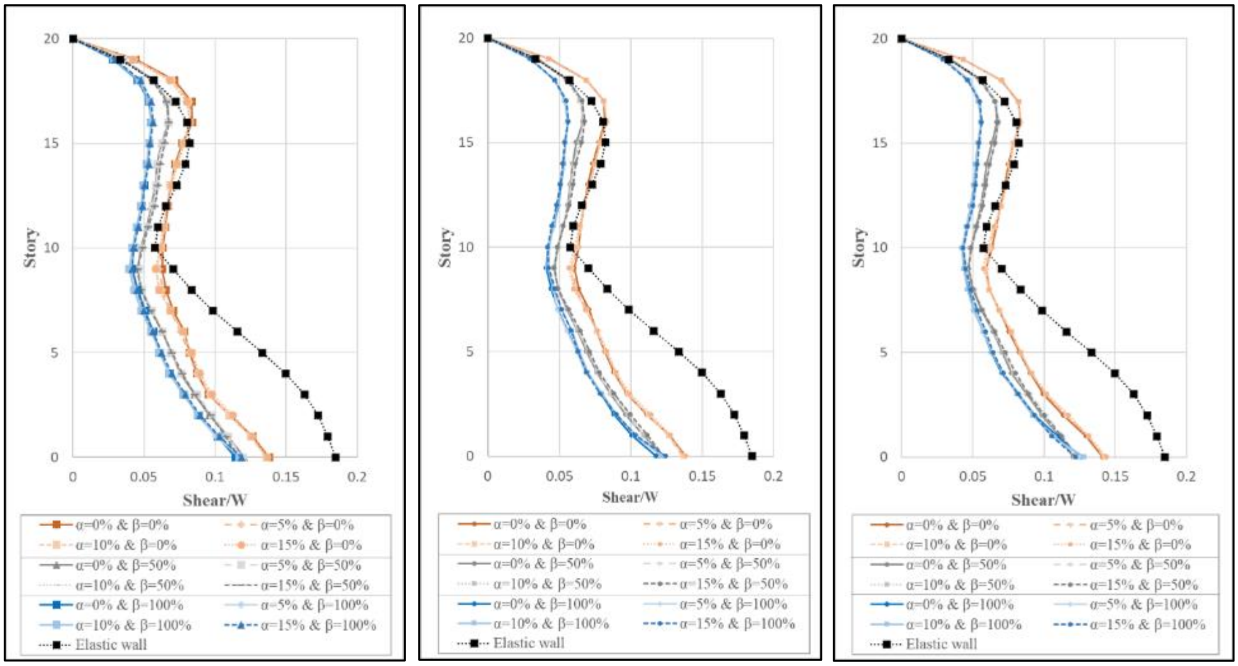

(a) *(b)* *(c)*

Figure 13. Comparing shear force distribution for all scenarios: (a) PT initial= 0%W; (b) PT initial= 7.5%W; (c) PT initial= 15%W

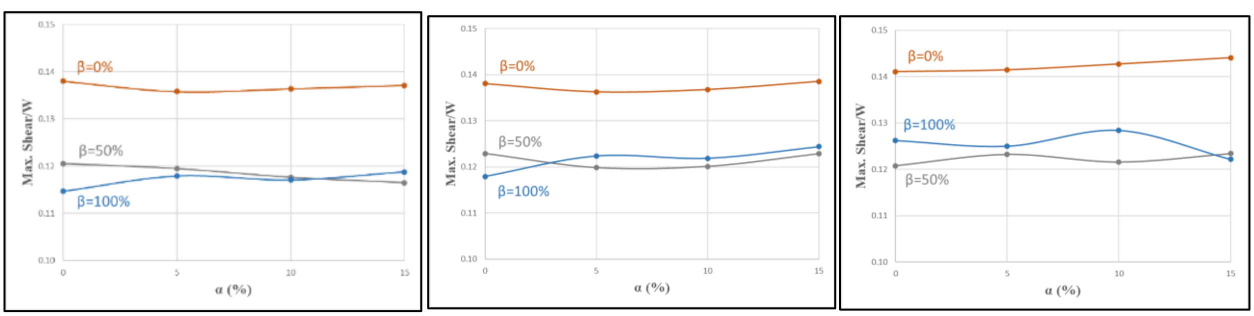

(a) *(b)* *(c)*

Figure 14. Comparing maximum shear force of the wall for all archetypes; (a) PT initial= 0%W; (b) PT initial= 7.5%W; (c) PT initial= 15%W

Moment

Figure 15 shows the mean values of the maximum moment normalized by the base moment of the building in different stories. All scenarios, including fixed elastic wall and UPT-PC walls, were normalized with the base moment (M_{rb}) compared in three groups with different PT initial forces (0%W, 7.5%W, and 15%W) and summarized in Figure 16 for the maximum moment in all stories. As discussed in previous sections, there was a moment redistribution among the stories due to the plastic hinge at the toe of the wall in UPT-PC walls compared to the elastic wall. So, the moment demands increased significantly in the middle stories than in the base. It means that the middle part of the shear wall can become the second plastic hinge zone. The highest values of the moment demand occurred in the structures with zero ED (β=0%), which were 1.86M_{base}, 1.8 M_{base}, and 1.72 M_{base} for PT initial forces equals 0%, 7.5%, and 15%, respectively. In addition, the lowest moment demand among all archetypes belongs to the structure with β=100%, α=15%, and PT initial force=15%, equal to 1.29 times M_{base}.

Generally, increasing all three structural parameters, α, β, and PT initial forces, mitigated the higher mode effects. ED (β) was the most influential parameter, so by increasing β from 0% to 100%, the maximum reduction of the moment demand was about 28%. This mitigation was 12% and 8% for PT initial forces and α, respectively, by increasing these parameters from 0% to 15%. The comparison of the slope of the curves in Figure 16 indicates that the most significant influence of α was related to the structure with 0% PT initial force.

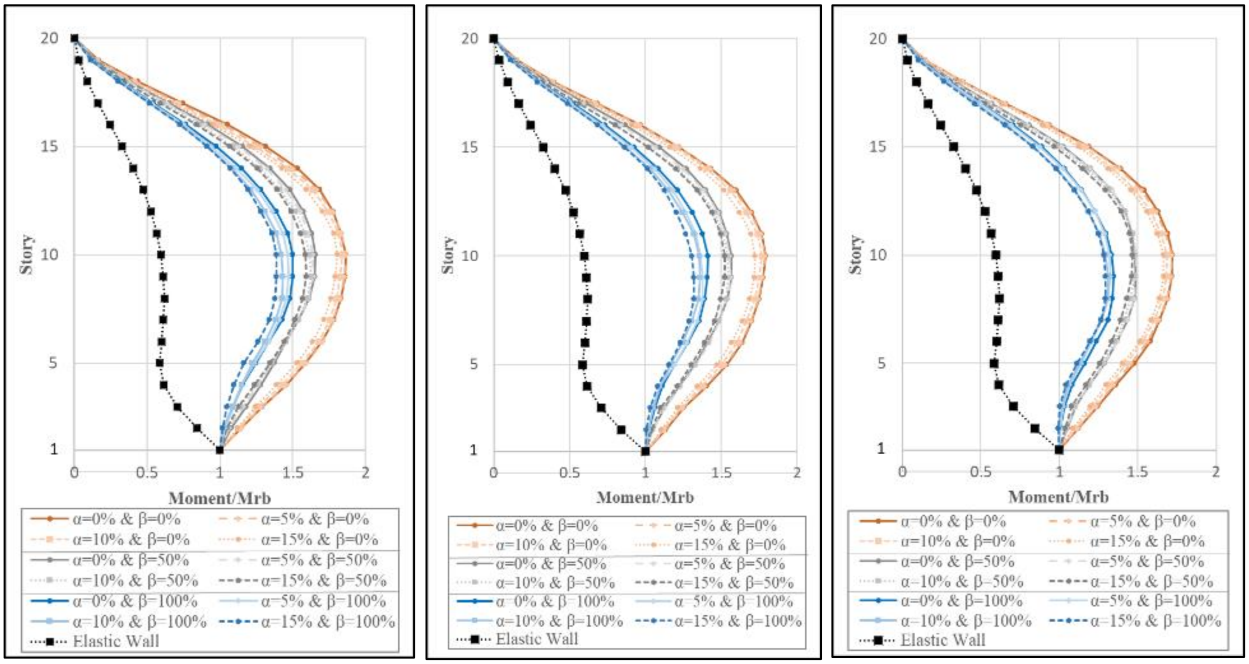

(a) *(b)* *(c)*

Figure 15. Comparing moment distribution for all scenarios: (a) PT initial= 0%W; (b) PT initial= 7.5%W; (c) PT initial= 15%W

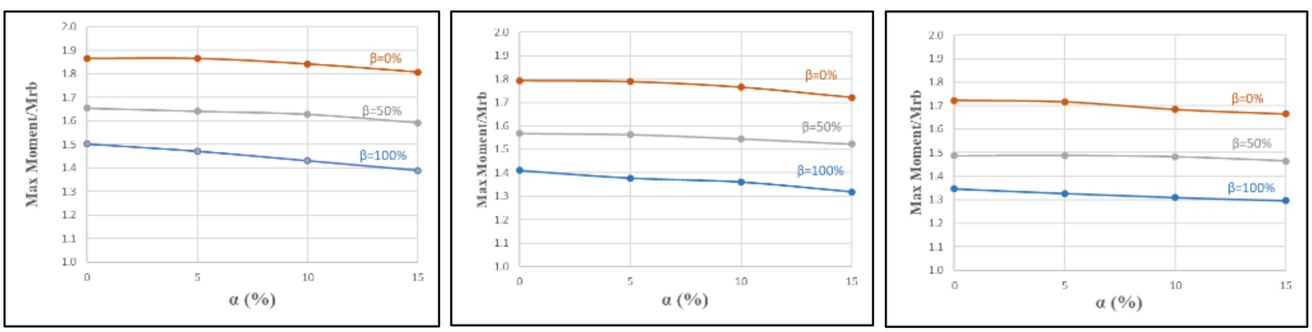

(a) *(b)* *(c)*

Figure16. Comparing maximum moment of the wall for all archetypes; (a) PT initial= 0%W; (b) PT initial= 7.5%W; (c) PT initial= 15%W

Acceleration

The presence of energy dissipation mechanisms can cause a more intense rocking motion, resulting in higher levels of acceleration and drift in the rocking wall. Like the results of drift distribution, the acceleration values of stories 1-8, as shown in Figure 1, in UPT-PC walls were noticeably higher than in the elastic shear wall. The minimum acceleration demand of the first story among all prototypes of the UPT-PC walls was 1.4 g. In all UPT-PC walls, the highest acceleration demand, observed in the first story, was reduced drastically in the 3rd story. Stories 4 to 20 had a uniform acceleration distribution in the height of the wall.

By increasing the EDs (β) in the UPT-PC walls, the acceleration of the lower stories can increase considerably. For example, Figure 18-c illustrates that enhancing β from 0% to 100% increased the maximum acceleration, which occurred in the first story, by about 50%. However, in story 20, the acceleration was reduced by 33% by improving ED from 0% to 100%, as shown in Figure 17-c. Overall, the highest and lowest values of maximum acceleration belong to the structures with β equal to 100% and 50%, respectively. So, the values of ED ratios should be optimized according to the characteristics of the UPT-PC walls. Regarding the other parameters, α and PT initial forces, although α does not significantly affect maximum acceleration, PT initial forces can affect the UPT-PC wall maximum acceleration noticeably, especially in higher ED values. Figure 18 shows that in the structure with β=100%, increasing PT initial forces from 0% to 15% raised the maximum acceleration by 13%.

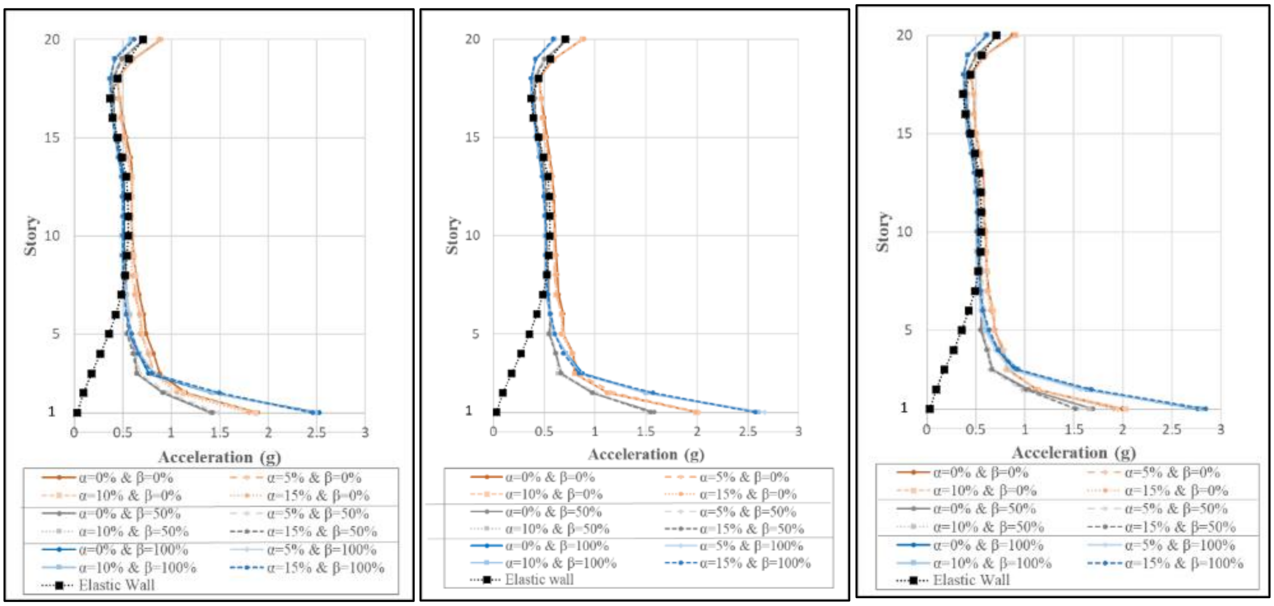

(a) (b) (c)

Figure 17. Comparing moment distribution for structural parameters: (a) α factor; (b) β factor; (c) Initial PT force

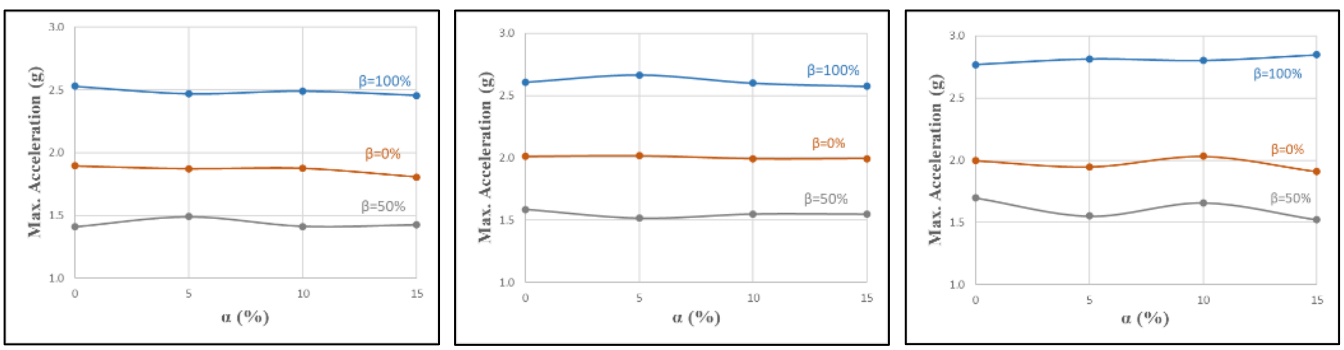

(a) (b) (c)

Figure 18. Comparing moment distribution for structural parameters: (a) α factor; (b) β factor; (c) Initial PT force

CONCLUSIONS

This paper conducted a parametric study to investigate the seismic response of UPT-PC wall systems and the higher-mode amplification effects of structural parameters on the higher modes. For this aim, various parameters, including strain hardening of PT tendons (α), the initial force of PT, and ED (β), were considered to be investigated through the nonlinear time history analysis.

The β parameter has the most significant influence on mitigating the amplification of mid-height moment demand in UPT-PC walls. Increasing ED (β) can decrease the maximum moment of these structures up to about 30% among all considered archetypes. It can also reduce the other demands such as shear forces, drift, and acceleration up to 15%, 25%, and 33%, respectively. However, the results showed that improving ED does not mitigate the demands in all cases. In the case of acceleration, it caused an increase in the acceleration of lower stories. Also, there was a fluctuation in the reduction of shear forces, so that β parameter should be optimized for higher values.

The two other parameters, α and PT initial force, do not have considerable effective mitigation on the higher mode effects. However, enhancing PT initial force reduces the moment demands and increases shear forces and acceleration of lower stories. In addition, α reduced the moment demands by up to 10% in the structures with 0% PT initial forces.

Overall, enhancing the ED is a practical approach to mitigate the higher-mode effects in the structural response of UPT-PC structures.

REFERENCES

[1] Bournas, DA., Negro, P., and Taucer FF. (2014). "Performance of industrial buildings during the Emilia earthquakes in Northern Italy and recommendations for their strengthening". Bulletin of Earthquake Engineering. 12(5): 2383-2404.

[2] Toniolo, G., and Colombo, A. (2012). "Precast concrete structures: the lessons learned from the L'Aquila earthquake". Structural Concrete. 13(2): 73-83.

[3] Priestley., M.J.N. (1996). “The PRESSS program: Current status and proposed plans for phase III”. PCI Journal 41: 22-40. DOI:10.15554/PCIJ.03011996.22.40.

[4] Kurama, Y., Pessiki, S., Sause, R., Lu, L.W. (1999). “Seismic Behavior and Design of Unbonded Post-Tensioned Precast Concrete Walls”. PCI Journal, V. 44, No.3.

[5] Erkmen, B., and Schultz, A.E. (2009). “Self-Centering Behavior of Unbonded, Post-Tensioned Precast Concrete Shear Walls, Journal of Earthquake Engineering”. 13:7, 1047-1064, DOI: 10.1080/13632460902859136

[6] Henry, R.S., Ingham, J.M. (2011). "Behaviour of tilt-up precast concrete buildings during the 2010/2011 Christchurch earthquakes". Structural Concrete. 12(4): 234-240.

[7] Belleri, A., Schoettler, M.J., Restrepo, J.I., Fleischman, R.B. (2014). “Dynamic behavior of rocking and hybrid cantilever walls in a precast concrete building”. ACI Structural Journal, 111 (3), pp. 661-671.

[8] Holden, T., Restrepo, J., Mander, J.B., (2003). “Seismic performance of precast reinforced and prestressed concrete walls”. J Struct Eng 129(3):286‑296.

[9] Perez, F.D.J. (1998). “Lateral load behavior and design of unbonded post- tensioned precast concrete walls with ductile vertical joint connectors”. PCI Journal, 136918608.

[10] Grigorian, M., Moghadasi, M.S., (2017). “Introducing a new wall- frame earth quake resisting system”..Asian jornal of civil engineering(BHRC) vol.18, No.3.

[11] Masroma, M.A., Abdul Hamid, N.H., (2020). “Review on the rocking wall systems as a self-centering mechanism and its interaction with floor diaphragm in precast concrete structures”. Latin American journal of solid and structures, 17(6), e291. http://dx.doi.org/10.1590/1679-78256115.

[12] Wiebe, L., Christopoulos, C., (2009). “Mitigation of higher mode effects in base-rocking systems by using multiple rocking sections”. J Earthq Eng 13(1 SUPPL. 1):83‑108.

[13] Khanmohammadi, M., Heydari, S., (2015). “Seismic behavior improvement of reinforced concrete shear wall buildings using multiple rocking systems”. Eng Struct 100:577‑589.

[14] Broujerdian, V., Mohammadi Dehcheshmeh, E., (2022). “Locating the rocking section in self-centering bi-rocking walls to achieve the best seismic performance”. Bulletin of Earthquake Engineering 20:2441–2468 https://doi.org/10.1007/s10518-022-01325-y.

[15] Priestley., M.J.N. (1991). “Overview of PRESSS research program”. PCI Journal 36:50–57. https://doi.org/10.15554/pcij.07011991.50.57.

[16] Pennucci, D., Calvi, G.M., Sullivan, T.J., (2009). “Displacement-based design of precast walls with additional dampers”. J Earthq Eng 13(S1):40‑65.

[17] Kurama, Y.C., (2005). “Seismic design of partially post-tensioned precast concrete walls”. PCI Journal 50:100–125. https://doi.org/10.15554/pcij.07012005.100.125.

[18] Masrom, M., Abdul Hamid, N., (2020). “Review on the rocking wall systems as a self-centering mechanism and its interaction with floor diaphragm in precast concrete structures”. Latin American Journal of Solids and Structures, doi.org/10.1590/1679-78256115.

[19] Weldon, B.D., Kurama, Y.C. (2012). “Analytical modeling and design validation of posttensioned precast concrete coupling beams for seismic regions”. Journal of Structural Engineering 1:224–234. https://doi.org/10.1061/(ASCE)ST.

[20] Canadian Precast/PrestressedConcrete Institute, (2021). “Total precast concrete high rise building design example”.

[21] McKenna, F., Fenves, G., Scott, M., (2000) “Open system for earthquake engineering simulation”. Berkeley, CA: University of California. http://opensees. berkeley.edu.

[22] Applied Technology Council. (2009). “Quantification of building seismic performance factors, FEMA Report P695”. Washington, DC, United States: Federal Emergency Management Agency.